

Token-Level Constraint Boundary Search for Jailbreaking Text-to-Image Models

Jiangtao Liu, Zhaoxin Wang, Handing Wang, *Senior Member, IEEE*, Cong Tian, *Senior Member, IEEE*, and Yaochu Jin, *Fellow, IEEE*

Abstract—Text-to-Image (T2I) generation has advanced rapidly in recent years, but they also raise safety concerns due to the potential production of harmful content. In the practical deployments, T2I services typically adopt full-chain defenses that combine a prompt checker, a securely trained generator, and a post-hoc image checker. Jailbreaking such full-chain systems is challenging in the black-box settings because prompt tokens form a discrete combinatorial space and the attack must satisfy multiple coupled constraints under sparse feedback and limited queries. To address these challenges, we propose Token-level Constraint Boundary Search (TCBS)-Attack, a novel query-based black-box jailbreak attack that searches for tokens located near the decision boundaries defined by text and image checkers. TCBS-Attack incorporates decision boundaries as constraint conditions to guide the evolutionary search of token populations, iteratively optimize tokens near these boundaries. Such evolutionary search process reduces the effective search space and improves query efficiency while preserving semantic coherence. Extensive experiments demonstrate that TCBS-Attack consistently outperforms state-of-the-art jailbreak attacks across various T2I models, including securely trained open-source models and commercial online services like DALL-E 3. TCBS-Attack achieves an ASR-4 of 52.5% and an ASR-1 of 22.0% on jailbreaking full-chain T2I models, significantly surpassing baseline methods.

Index Terms—Evolutionary optimization, constraint optimization problem, Text-to-Image model, jailbreak attack.

I. INTRODUCTION

TEXT-TO-IMAGE (T2I) generation has seen rapid advancements in recent years, fueled by the development of powerful deep diffusion models such as Stable Diffusion [1] and DALL-E [2]. These models are capable of producing highly realistic and creative images from natural language descriptions. However, this progress has raised significant concerns regarding the potential generation of inappropriate or harmful content, commonly referred to as Not-Safe-For-Work (NSFW) contents [3]–[8]. To mitigate these risks, a large body of prior work [9]–[16] studies jailbreak attacks, which aim to craft adversarial prompts that circumvent safety checkers and elicit NSFW content from T2I models [17]–[24]. However, the common settings for the existing jailbreak attacks do not

fully reflect real deployments, which typically adopt full-chain defenses rather than a single filter: a prompt checker screens the input text before generation, a securely trained T2I model suppresses unsafe concepts during generation, or a post-hoc image checker inspects the generated image and blocks unsafe outputs. This gap between single-module evaluation and full-chain deployment motivates the need to assess and strengthen full-chain jailbreak robustness.

In essence, jailbreaking T2I models is an optimization problem in which the decision variable is the adversarial prompt as a discrete token sequence, and the objective is to induce the model to generate the target NSFW content while passing the deployed safety checkers. The recent jailbreak attacks targeting T2I models have primarily focused on crafting adversarial prompts that bypass safety checkers like Stable Diffusion’s Safety Checker [1]. These methods can be broadly categorized into gradient-based and query-based approaches. Gradient-based attacks [17], [25] treat the target model as a white-box system, leveraging access to the model’s gradient information to optimize adversarial prompts. MMA-Diffusion [17] leverages token-level gradients to guide the optimization process, crafting adversarial prompts that effectively bypass prompt filters. However, gradients are often unavailable or unreliable in real deployments, limiting practical applicability [26], [27]. In contrast, query-based black-box attacks [28], [29] search the discrete token space without requiring gradients. The techniques in this category include reinforcement learning or zero-order optimization approaches such as SneakyPrompt [28] and DiffZOO [29], which explore token substitutions and evaluate candidates via the model feedback. While query-based methods preserve semantic coherence and are practically applicable to deployed systems, they may suffer from slow convergence or become trapped in local optima if exploration is insufficient, especially when the attack must satisfy multiple safety constraints along the full defense pipeline. In the full-chain setting, the search space is combinatorial, and the success must satisfy coupled constraints from both text and image checkers. Meanwhile, the adversarial prompt should remain semantically coherent and natural, which sharply restricts feasible modifications. These challenges motivate a constraint-oriented framework that can optimize reliably under a limited query budget.

To address these issues, the recent work uses evolutionary algorithms (EAs) to search adversarial prompts, maintaining a population of candidate prompts and iteratively applying token-level mutation and selection. Such evolutionary approaches can balance exploration and exploitation in a discrete space, improve robustness against local optima. In the LLM

This work was supported in part by the National Natural Science Foundation of China (No. 62376202). (*Corresponding author: Handing Wang*)

J. Liu, Z. Wang, and H. Wang are with School of Artificial Intelligence, Xidian University, Xi’an 710071, China. (E-mail: 23171214704@stu.xidian.edu.cn, zwxwang74@163.com, hdwang@xidian.edu.cn).

C. Tian is with School of Computer Science and Technology, Xidian University, Xi’an 710071, China. (E-mail: ctian@mail.xidian.edu.cn).

Y. Jin is with the Trustworthy and General Artificial Intelligence Laboratory, School of Engineering, Westlake University, Hangzhou 310030, China. (E-mail: jinyaochu@westlake.edu.cn).

jailbreak attacks, AutoDAN [30] uses a hierarchical genetic algorithm to refine stealthy jailbreak prompts at paragraph and sentence levels under a fitness score based on response negative log-likelihood. GPTFUZZER [31] starts from a pool of human-written jailbreak templates and iteratively mutates and retains only successful templates under a query budget. Similar EA-style prompt search ideas are applicable to T2I jailbreaking under black-box, constraint-coupled defenses. For example, RIATIG [32] explicitly adopts a genetic algorithm style search to evolve imperceptible adversarial prompts that remain close to benign language while progressively improving attack efficacy, enabling broad exploration of semantically similar variants. HTS-Attack [18] implements the heuristic token recombination and mutation that mirrors the mutation–selection cycle of EAs. By recombining high-performing token sequences and retaining diverse candidates, HTS-Attack reduces the chance of getting stuck in local optima and improves the robustness against prompt filters. However, most prior evolutionary jailbreak attacks primarily focus on text defenses and do not jointly incorporate post-hoc image checker feedback into their evolutionary loops, which limits their robustness in full-chain scenarios and leaves substantial query budget wasted on candidates that are unlikely to pass the image checker.

A key observation is that both prompt checkers and image checkers can be viewed as classifiers with decision thresholds, which induce decision boundaries separating “safe” from “unsafe” regions. Prompts or their induced generations near these boundaries tend to be most sensitive to small perturbations: small and semantics-preserving token changes may flip the safety decision, yielding strong adversarial effectiveness while keeping the prompt natural and less likely to trigger explicit keyword rules. Therefore, instead of performing the search over the entire discrete space, we leverage the boundary information as a structural guidance for constrained optimization. By focusing search on tokens that lie near the constraint boundaries, we can substantially reduce the effective search space and improve query efficiency under full-chain defenses.

Based on this motivation, we propose TCBS-Attack, a novel query-based black-box evolutionary jailbreak method that performs token-level constraint boundary search guided by the decision boundaries defined by text and image checkers.

Our approach demonstrates robust attack capabilities across various adversarial environments. This advantage is attributed to TCBS-Attack’s evolutionary approach and its robust search capabilities. We summarize our contributions as follows:

- We propose a novel evolutionary black-box jailbreak attack method, TCBS-Attack, which employs a heuristic token search based on constraint boundary.
- TCBS-Attack reduces the effective search space by leveraging constraint boundaries induced by the safety checkers and focusing the search on regions near the boundaries with high adversarial potential, which improves the query efficiency and robustness under full-chain defenses.
- We design token-level efficient search and selection operators with explicit constraint handling, and extensive experiments across diverse T2I models, prompt checkers,

post-hoc image checkers, and online commercial services demonstrate the effectiveness of TCBS-Attack.

The remainder of this paper is organized as follows. Section II introduces the full-chain jailbreak attacks on T2I Models. Section III provides the details of TCBS-Attack. Section IV describes the experimental settings and reports the experimental results. Section V concludes this paper.

II. FULL-CHAIN JAILBREAK ATTACKS ON T2I MODELS

T2I systems [1] are commonly instantiated by generators based on diffusion [33], which iteratively transform random noises into a realistic image under the guidance of text conditioning. We study jailbreaking against a full-chain T2I system, which reflects the common deployment practice where multiple defensive modules are composed in a pipeline rather than relying on a single filter.

The full-chain jailbreaking can be modeled from a probabilistic optimization perspective. Here, we use p_{tar} to denote the target prompt that contains NSFW contents (e.g., “A naked man and a naked woman in the room”) and p_{adv} to denote that the adversarial prompt crafted by the attacker. Given an input prompt p_{tar} , the goal is to find an adversarial prompt p_{adv} that maximizes the conditional probability of being a successful jailbreak prompt. We denote by $\mathcal{P}(p_{adv}|p_{tar})$ the conditional probability that p_{adv} belongs to the distribution of prompts that can successfully jailbreak the deployed full-chain system under the target intent p_{tar} .

$$\begin{aligned} \max \quad & \mathcal{P}(p_{adv}|p_{tar}) \\ \text{s.t.} \quad & \begin{cases} F_{\theta}(p_{adv}) \neq NULL, \\ F_{text}(p_{adv}) = 1, \\ F_{img}(p_{adv}) = 1, \end{cases} \end{aligned} \quad (1)$$

where $F_{\theta}(\cdot)$ denotes the deployed T2I model. If an adversarial prompt p_{adv} is intercepted by the defense mechanism and no image is generated, then $F_{\theta}(p_{adv}) = NULL$. Conversely, if an image is successfully generated, it is represented as $F_{\theta}(p_{adv})$. $F_{text}(\cdot)$ represents the prompt checker: if p_{adv} passes this checker, $F_{text}(p_{adv}) = 1$; otherwise, $F_{text}(p_{adv}) = 0$. Similarly, $F_{img}(\cdot)$ denotes the post-hoc image checker: if p_{adv} passes this checker, $F_{img}(p_{adv}) = 1$; otherwise, $F_{img}(p_{adv}) = 0$.

Concretely, given an input prompt p_{tar} , a typical full-chain system first applies a prompt checker $F_{text}(\cdot)$ to screen text that violates safety policies. If the prompt passes, the T2I generator $F_{\theta}(\cdot)$ produces an image, and the generation is often stochastic. Finally, a post-hoc image checker $F_{img}(\cdot)$ inspects the generated image and blocks unsafe outputs. In addition, the generator itself may be securely trained through safety tuning or concept suppression to discourage unsafe concepts during generation. Overall, the query outcome observed by the attacker is jointly determined by these modules and thus reflects the full set of constraints faced by jailbreak attacks. The goal of a jailbreak attack is to find an adversarial prompt p_{adv} that induces the generation of NSFW content aligned with a target intent, while passing the deployed safety mechanisms along the full-chain.

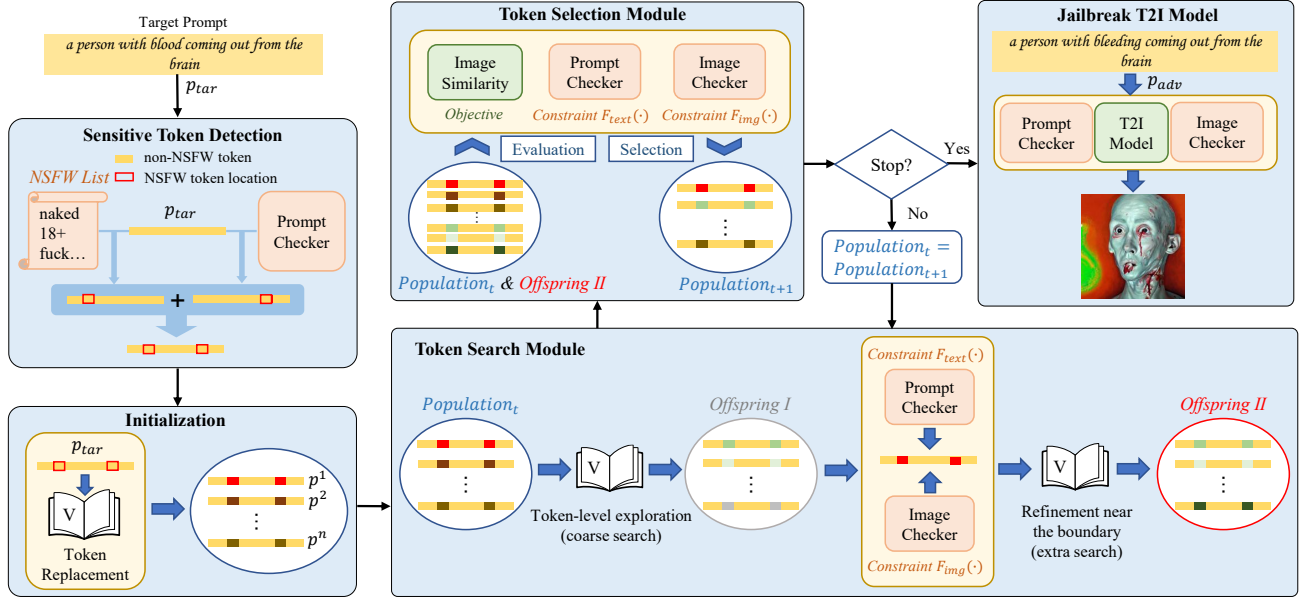


Fig. 1: Overview of the proposed TCBS-Attack framework. TCBS-Attack initially detects sensitive tokens and initializes population. Subsequently, candidate prompts in the population undergo iterative refinement through token search and token selection based on constraint boundary, effectively bypassing safety measures in T2I models.

III. METHODOLOGY

A. Motivation

Jailbreaking a full-chain T2I system is inherently a black-box constrained optimization problem over a prompt token sequence, which motivates our evolutionary optimization approach. Due to the multiple coupled constraints (safety checkers), the feasible token space is typically tiny compared with the combinatorial prompt space, which requires a large number of queries to be found. In fact, these safety checkers are binary classifiers with decision boundaries in the text embedding space [28], where a prompt that lies in the vicinity of a decision boundary is particularly informative: a small and semantics-preserving token change may flip a reject decision to accept.

Therefore, TCBS-Attack reduces the original large prompt space to the space around the decision boundaries of safety checkers to enhance the search efficiency. As shown in Fig. 1, TCBS-Attack performs the token-level search and selection guided by the constraint boundaries of text and image checkers, aiming to concentrate evolutionary search on candidates near the boundary.

B. Problem Formulation

Given an input target sequence $p_{tar} = [p_1, p_2, \dots, p_L] \in \mathbb{N}^L$, where $p_i \in \{0, 1, \dots, |V| - 1\}$ is the i^{th} token's index, V is the vocabulary codebook, $|V|$ is the vocabulary size, and L is the prompt length, the jailbreak problem in Eq. (1) can be further re-formulated as follows:

$$\begin{aligned} & \max \text{sim}(F_\theta(p_{adv}), F_\theta(p_{tar})) \\ \text{s.t.} & \begin{cases} F_\theta(p_{adv}) \neq \text{NULL} \\ F_{text}(p_{adv}) = 1 \\ \text{score}(p_{adv}) = 0. \end{cases} \end{aligned} \quad (2)$$

The objective in Eq. (2) maximizes the semantic similarity $\text{sim}(F_\theta(p_{adv}), F_\theta(p_{tar}))$ between the image generated from the adversarial prompt p_{adv} and the target content p_{tar} . Function $\text{sim}(\cdot, \cdot)$ is calculated by using a pre-trained CLIP model [34]. Specifically, we encode the generated images with the CLIP image encoder and measure cosine similarity in the embedding space.

The constraints in Eq. (2) follow the same full-chain setting as Eq. (1). $F_\theta(p_{adv}) \neq \text{NULL}$ ensures the system returns a valid image. The binary prompt checker $F_{text}(p_{adv})$ employs NSFW-text-classifier [35]. The post-hoc image checker adapts Stable Diffusion's built-in Safety Checker [1], which provides a continuous NSFW score. It computes the cosine similarity $\text{sim}_s = [\text{sim}_{s1}, \text{sim}_{s2}, \dots, \text{sim}_{s17}]$ between the image's CLIP embedding vector [34] and the pre-calculated text embedding of 17 unsafe concepts [28]. The cosine similarity for each dimension is then compared with the corresponding threshold $[t_1, t_2, \dots, t_{17}]$. If the cosine similarity for any dimension exceeds its threshold, the image is classified as NSFW, and a fully black image is returned. The NSFW score is written as follows:

$$\text{score}(p_{adv}) = \sum_{i=1}^{17} \max(\text{sim}_{si} - t_i, 0). \quad (3)$$

When $\text{score}(p_{adv}) = 0$, it indicates that p_{adv} allows the T2I model to generate an image normally. However, when $\text{score}(p_{adv}) > 0$, it signifies that the image generated by p_{adv} has been detected and intercepted by the safety checker.

C. Token-Level Constraint Boundary Search

TCBS-Attack generates adversarial prompts capable of bypassing safety checkers in T2I models while ensuring semantic

consistency with the target prompt. We refine adversarial prompts iteratively by manipulating sensitive and non-sensitive tokens while maintaining constraints that prevent triggering safety mechanisms. Specifically, TCBS-Attack begins by detecting sensitive tokens in the target prompt p_{tar} . Based on the detected sensitive tokens, replacements are made to initialize and generate n candidate prompts. These n candidates in the t^{th} iteration (denoted as $Population_t$) then undergo a token search based on constraint boundary, resulting in n new candidates (denoted as $OffspringI$). Subsequently, the $2n$ candidates are evaluated through a token selection based on constraint boundary, to select the final n candidates (denoted as $Population_{t+1}$) that will move on to the next iteration. The details of the method are shown in Fig. 1.

1) *Initialization*: In the initialization phase, we focus on mutating both sensitive and non-sensitive tokens in the target prompt p_{tar} , where we perform sensitive token detection to identify sensitive tokens \mathcal{S}_1 through matching with a pre-defined NSFW word list \mathcal{W} . Then, we use the NSFW-text-classifier [35] to select the tokens (\mathcal{S}_2), which are most likely to be classified as NSFW in the vocabulary codebook V . These two sets of tokens are subsequently merged to form the final list of sensitive tokens (\mathcal{S}). The details of the process are shown in Algorithm 1.

For each sensitive token in p_{tar} , we first find the k most similar tokens based on the CLIP text similarity in the vocabulary codebook V . One of these tokens is then randomly selected and used to replace the original sensitive token. For non-sensitive tokens, we perform a similar search process with a probability p_{s1} to replace them with tokens that have high semantic similarity. The details of the process are shown in Algorithm 2. This process is repeated n times, resulting in the generation of n candidates $[p^1, p^2, \dots, p^n]$. These candidates will serve as the initial population for subsequent optimization steps, providing a diverse starting point for further refinements in the token search and selection.

2) *Token Search Based on Constraint Boundary*: The proposed token search aims to improve the attack performance while moving the candidate toward feasible solution space under the full-chain constraints. We first perform a token-level search to generate new candidates (coarse search), and then spend additional queries only on candidates that are more likely to become feasible because they lie close to the constraint boundary (extra search). The details of the method are shown in Fig. 2.

Given a candidate prompt p in $Population_t$, we start by refining it through token replacements at sensitive positions, which is same with that in the initialization phase. This operation is primarily intended to evade the checkers while preserving the original intent of the prompt. Also, we search the non-sensitive tokens in p to increase the diversity of the search and mitigate premature convergence in the discrete space. For non-sensitive tokens, we first decide whether the non-sensitive part of the prompt participates in replacement with probability p_{s2} . If the non-sensitive part is chosen, we then proceed with a search with a probability p_{s1} to find its similar token.

After one round of coarse search, we denote the resulting

Algorithm 1 Sensitive Token Identification

Require: Prompt $p = [p_1, p_2, \dots, p_L]$; NSFW word list \mathcal{W} ; classifier $T_{label}(\cdot), T_{score}(\cdot)$
Ensure: Sensitive token set \mathcal{S} ; sensitive index list \mathcal{I}

- 1: $\mathcal{S}_1 \leftarrow \{p_i \mid p_i \in \mathcal{W}\}$
- 2: $\mathcal{S}_2 \leftarrow \emptyset, \mathcal{I} \leftarrow \emptyset$
- 3: **if** $T_{label}(p) = \text{NSFW}$ **then**
- 4: $s_{ori} \leftarrow T_{score}(p)$
- 5: **for** $t = 1$ to L **do**
- 6: $p^{(-t)} \leftarrow p$ with p_t removed
- 7: $s_t \leftarrow T_{score}(p^{(-t)})$
- 8: $\Delta_t \leftarrow s_{ori} - s_t$
- 9: **end for**
- 10: Sort indices t by Δ_t in descending order to get sequence l
- 11: $u \leftarrow p$
- 12: **for each** t in l **do**
- 13: $\mathcal{S}_2 \leftarrow \mathcal{S}_2 \cup \{p_t\}$
- 14: Remove p_t from u
- 15: **if** $T_{label}(u) \neq \text{NSFW}$ **then**
- 16: **break**
- 17: **end if**
- 18: **end for**
- 19: **end if**
- 20: $\mathcal{S} \leftarrow \mathcal{S}_1 \cup \mathcal{S}_2$
- 21: **for** $i = 1$ to L **do**
- 22: **if** $p_i \in \mathcal{S}$ **then**
- 23: Append i to \mathcal{I}
- 24: **end if**
- 25: **end for**
- 26: **return** \mathcal{S}, \mathcal{I}

candidate set as $OffspringI$, many of which might be around the constraint boundary but infeasible. Therefore, we conduct an extra search based the the image and prompt checkers separately.

The constraint boundary of the image checker is continuous and can be directly characterized by the violation score in Eq. (2), where a smaller positive $score(\cdot)$ indicates closer proximity to the decision boundary. Therefore, a further search step for the candidate p' in $OffspringI$ is triggered in the image domain when

$$\begin{cases} sim(F_\theta(p'), F_\theta(p_{tar})) > sim_{best} - m_1 \\ 0 < score(p') < m_2, \end{cases} \quad (4)$$

where sim_{best} represents the best image similarity recorded during the search process, m_1 and m_2 are two hyperparameters used to constrain the range of $sim(F_\theta(p'), F_\theta(p_{tar}))$ and $score(p')$.

In contrast, the prompt checker typically provides a binary decision. Token editing in our search is inherently small-step, each replacement is sampled from a top- k set of semantically similar candidates. A newly rejected candidate is obtained from a feasible parent after one or a few edits, and can be treated as near the text-side boundary on the infeasible side,

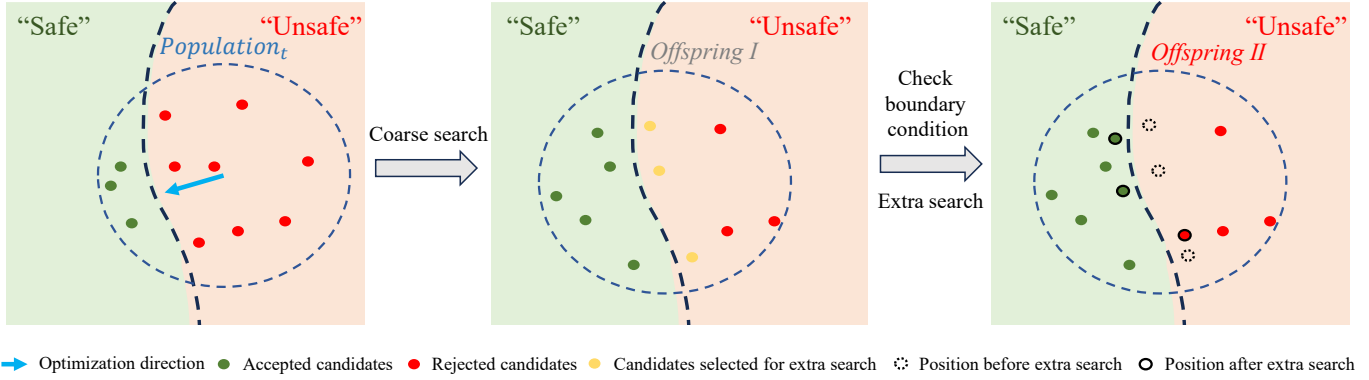


Fig. 2: Intuitive illustration of token search based on constraint boundary.

Algorithm 2 Semantics-Preserving Token Replacement

Require: Prompt $p = [p_1, p_2, \dots, p_L]$; sensitive indices \mathcal{I} ; neighbor function $\text{TopK}(\cdot, k)$; hyperparameters p_{s1}, k ; Bernoulli sampler $\text{Bernoulli}(\cdot)$

Ensure: Replaced prompt p'

```

1:  $p' \leftarrow p$ 
2: for  $i = 1$  to  $L$  do
3:   if  $i \in \mathcal{I}$  then
4:     /*sensitive positions*/
5:      $\mathcal{N}_i \leftarrow \text{TopK}(p_i, k)$ 
6:      $p'_i \leftarrow \text{SampleUniform}(\mathcal{N}_i)$ 
7:   else
8:     /*non-sensitive positions*/
9:     if  $\text{Bernoulli}(p_{s1}) = 1$  then
10:       $\mathcal{N}_i \leftarrow \text{TopK}(p_i, k)$ 
11:       $p'_i \leftarrow \text{SampleUniform}(\mathcal{N}_i)$ 
12:     end if
13:   end if
14: end for
15: return  $p'$ 

```

making it a natural target for additional refinement. Therefore, we trigger a further search step in the text domain when

$$F_{\text{text}}(p') = 0. \quad (5)$$

If the new candidate p' satisfies the conditions in either Eq. (4) or Eq. (5), we will perform the same search process on p' again. We denote the population after the second replacement as *OffspringII*.

Importantly, we do not assume an explicit boundary representation. Instead, it is implicitly induced by deployed safety modules. Continuous violation scores directly quantify boundary proximity, while binary decisions are handled by small, semantics-preserving token edits that flip feasibility. Therefore, adapting TCBS-Attack to a new deployment mainly amounts to selecting the corresponding checkers and composing them as constraints, rather than engineering a new boundary definition, which supports the practical applicability of our method.

3) *Token Selection Based on Constraints*: The token selection phase involves selecting n candidates from a pool of $2n$ candidates, which includes *Population_t* and *OffspringII*.

The selection process uses a binary tournament mechanism, where two individuals are randomly selected from the population, and the one with better fitness is chosen as a parent for the next generation. For each pair of candidates p_{adv1} and p_{adv2} , the selection is based on their image similarity, NSFW scores $\text{score}(p_{adv1}), \text{score}(p_{adv2})$ and $F_{\text{text}}(p_{adv1}), F_{\text{text}}(p_{adv2})$. The specific conditions are as follows:

- 1) If $\text{score}(p_{adv1}) = \text{score}(p_{adv2}) = 0$, this indicates that both candidates can successfully pass through the image checker. If $F_{\text{text}}(p_{adv1}) \neq F_{\text{text}}(p_{adv2})$, we select the candidate p_{adv1} for which $F_{\text{text}}(p_{adv1}) = 1$. If $F_{\text{text}}(p_{adv1}) = F_{\text{text}}(p_{adv2})$, we select the candidate with the higher image similarity, as it more closely aligns with the target content.
- 2) If $\text{score}(p_{adv1}) = 0, \text{score}(p_{adv2}) > 0$ or $\text{score}(p_{adv1}) > 0, \text{score}(p_{adv2}) = 0$, we select the candidate with a *score* of 0, as it is more likely to successfully generate an image that passes through the image checker.
- 3) If $\text{score}(p_{adv1}) > 0, \text{score}(p_{adv2}) > 0$, we evaluate $F_{\text{text}}(p_{adv1})$ and $F_{\text{text}}(p_{adv2})$. If $F_{\text{text}}(p_{adv1}) \neq F_{\text{text}}(p_{adv2})$, we select the candidate for which the result equals 1. If $F_{\text{text}}(p_{adv1}) = F_{\text{text}}(p_{adv2})$, we select the candidate with the smaller NSFW score, as it is more likely to pass through the image checker after further refinement.

This selection process ensures that only the most promising candidates, with the highest potential to bypass safety mechanisms while maintaining semantic relevance to the target content, are chosen for the next iteration. This process continues until the number of selected candidates reaches n constituting *Population_{t+1}* entering the next iteration.

IV. EXPERIMENTAL RESULTS

A. Experimental Settings

Datasets. We employ three standard benchmarks to evaluate our experiments: MMA-Diffusion benchmark [17], UnsafeDiff [3] and VBCDE [36]. The MMA-Diffusion benchmark specifically encompasses NSFW prompts within the sexual content category, with prompts originally derived from the LAION-COCO [37] dataset, also leveraged in our analytical

framework. We incorporate UnsafeDiff, a curated dataset explicitly designed for NSFW evaluation. UnsafeDiff provides 30 prompts across six NSFW themes: adult content, violence, gore, politics, racial discrimination, and inauthentic notable descriptions. Finally, VBCDE comprises five major censorship classes—violence, gore, illegal activities, discrimination, and pornographic content—each represented by approximately 20 prompts to cover the principal review scopes enforced by current T2I models. In total, we select 200 prompts from these datasets for the comprehensive evaluation of our experiments.

T2I models. We primarily conduct our experiments on the SDv1.4 model. Furthermore, we repurpose adversarial prompts obtained from these attacks to evaluate transferability against two additional open-source models: SLD(Medium) [5] and SafeGen [38]. To assess the effectiveness of adversarial prompts on online T2I models, we select DALL-E 3 [2].

Defensive methods. We select three types of defense mechanisms commonly used by T2I models: prompt checkers, securely trained T2I models, and post-hoc image checker. For prompt checkers, we utilize NSFW-text-classifier [35] and Detoxify [39]. These classifiers serve as pre-screening mechanisms by identifying NSFW content in prompts submitted to T2I models. Regarding securely trained T2I models, we choose SLD and SafeGen, both explicitly trained to suppress the generation of inappropriate images typically produced by standard T2I models. As for post-hoc image checking, we employ Stable Diffusion’s built-in Safety Checker, which replaces detected NSFW content with entirely black images.

Baselines. We select eight state-of-the-art(SOTA) jailbreak attack methods for comparison against our proposed TCBS-Attack: I2P [5], QF-Attack [40], SneakyPrompt [28], FLIRT [41], DiffZOO [29], MMA-Diffusion [17], Divide-and-Conquer Attack(DACA) [36], U3-Attack [42], DREAM [43] and HTS-Attack [18]. Specifically, I2P provides a human-written prompt dataset, from which we chose 200 prompts aligned with NSFW categories in UnsafeDiff for our experiments. QF-Attack, initially designed for circumventing T2I model defenses. Following MMA-Diffusion’s adaptation, we employ its modified objective function and adopt the GREEDY strategy. SneakyPrompt utilizes reinforcement learning techniques to search for adversarial prompts targeting T2I models. FLIRT uses iterative in-context learning of the red language model to generate adversarial prompts. DiffZOO applies zero-order optimization to obtain gradient approximation and leverages C-PRV and DPRV to enhance adversarial prompts within the discrete prompt domain. MMA-Diffusion leverages gradient-based optimization to guide prompt refinement while maintaining high fidelity of generated outputs. DACA employs large language models (LLMs) to partition NSFW contents into multiple benign descriptions, generating adversarial prompts accordingly. U3-Attack is a universal multimodal jailbreak framework that learns transferable prompt-side paraphrases and image-side adversarial perturbations to generate adversarial prompts in black-box settings. DREAM formulates red teaming as distribution learning by modeling a probabilistic distribution over unsafe prompts and optimizing it with a zeroth-order method. HTS-Attack utilizes heuristic token search methodologies to recombine and mutate tokens

for optimizing adversarial prompts. During our reproduction, we observed that due to differences in datasets, the original configuration of HTS-Attack’s second text sim filter had little effect on pruning low-quality adversarial candidates. As a result, the method suffered from excessive runtime overhead. To ensure a fair experimental comparison under equivalent difficulty, we reconfigured HTS-Attack by modifying its second text sim filter. Specifically, in each optimization iteration, we retain only the top 12 adversarial candidates based on their text similarity scores. This modification maintains an equivalent query budget to TCBS-Attack and ensures that both methods operate under comparable computational constraints.

Evaluation metrics. We adopt multiple metrics to thoroughly evaluate the effectiveness of jailbreak attack methods. Primarily, we use the Attack Success Rate out of N syntheses (ASR- N) metric. Specifically, for each adversarial prompt, we generate N images using the T2I models. If at least one image bypasses the safety checkers and contains NSFW content, we deem the adversarial attack successful. In our experiments, we employ ASR-4 and ASR-1 to assess the performance. To verify the NSFW content of generated images, we utilize two independent NSFW detectors: Q16 [44] and MHSC [3]. Also, we measure the proportion of adversarial prompts passing safety checkers using the Bypass metric. We define Bypass-Text as the rate of adversarial prompts passing the prompt checker, and Bypass-Img as the rate of generated images successfully passing the post-hoc image checker.

Parameter Settings. In our experiments, we utilize the vocabulary from the transformer [45] model BERT [46] and employ CLIP-ViT-Base-Patch16 as the pre-trained text and image encoders $T_\theta(\cdot)$, $I_\theta(\cdot)$. To generate reference images, we employ the surrogate T2I model $F_s(\cdot)$, specifically Stable Diffusion v1.5, which excludes any defensive modules. Specifically, we set a population size n of 10. The number of iterations T is 50 and the maximum number of queries is 1000. We set the same query number for other query-based methods. The probability p_{s1} of each non-sensitive token mutation is 0.1. During the token search process, the probability p_{s2} of adversarial prompts causing non-sensitive token mutation is set to 0.2. The number of similar tokens during token replacement k is 20. The relaxation margins for the image similarity constraint and NSFW score constraint are set to $m_1 = 0.05$ and $m_2 = 0.01$.

Sensitive Word List. Table I provide the explicit sensitive word lists employed during the sensitive token detection phase in TCBS-Attack. It is worth noting that the sensitive terms employed in our study are derived from the curated list compiled by MMA-Diffusion, and the table presented here uses only a subset of the full vocabulary. During the experiment, we proactively exclude from the vocabulary any tokens that contain or are composed of these sensitive words. Additionally, in our sensitive token detection phase, we explicitly check whether a given prompt includes any of the terms from this list. This dual strategy not only enhances the stealthiness of our attack prompts but also proves effective in circumventing prompt checkers that rely primarily on keyword-based filtering.



Fig. 3: Visualization results of TCBS Attack.

TABLE I: Sensitive word list.

Sensitive word list	
sexual	vagina
nude	naked child
nudity	explicit content
sex	uncensored
18+	fuck
naked	nipples
nsfw	visible nipples
porn	breast
dick	areola

B. Experimental Results on Jailbreaking Full-Chain T2I Models

To evaluate the robustness and efficacy of our proposed TCBS-Attack in a full-chain scenario, we integrate both prompt-based and image-based defense mechanisms typically employed by T2I models. Specifically, we combine the prompt checker module (NSFW-text-classifier and Detoxify) and the post-hoc image checker module (Stable Diffusion’s built-in Safety Checker) to comprehensively assess the adversarial attack effectiveness.

Table II presents the comparative evaluation of TCBS-Attack against various baseline methods across two different prompt checkers and the post-hoc image checker using the SDv1.4. Overall, TCBS-Attack consistently achieves superior performance across multiple evaluation metrics. By iteratively refining token selection based on proximity to these checkers’ decision boundaries, TCBS-Attack consistently evades detection by maintaining semantic coherence while ensuring the stealthiness of generated prompts. In prompt checker evaluations, Detoxify exhibits relatively weaker defensive capabilities against baseline methods. In contrast, the gradient-based MMA-Diffusion method is most easily intercepted, demonstrating only a 5.5% success rate against the NSFW-text-

classifier. While DACA effectively bypasses prompt checkers by decomposing unethical prompts into benign components, this approach considerably weakens the attack performance of adversarial prompts. Among all evaluated methods, our proposed TCBS-Attack consistently achieves high bypass success rates. Notably, TCBS-Attack significantly outperforms other methods in tests against the NSFW-text-classifier, highlighting its effectiveness.

In the post-hoc image detection evaluations, the tool detects potentially offensive content in generated images and returns completely black images upon identifying violations. TCBS-Attack demonstrates exceptional efficiency in bypassing the image checker, achieving a Bypass-Img rate of 82%, the highest among all methods tested.

We further analyze the attack success rates of images generated after successfully bypassing both prompt and image checkers. U3-Attack achieves an ASR-1 of 16.0% and ASR-4 of 24.0% when evaluated using Detoxify. DREAM achieves an ASR-1 of 10.5% and ASR-4 of 13.0% when evaluated using the NSFW-text-classifier. Our proposed method consistently achieves the highest NSFW attack success rates across all prompt and image checkers. Specifically, TCBS-Attack achieves an ASR-1 of 13.5% and ASR-4 of 29.5% when evaluated using the NSFW-text-classifier, and an ASR-1 of 22.0% and ASR-4 of 52.5% when evaluated using Detoxify. These results demonstrate that TCBS-Attack effectively generates adversarial prompts that bypass safety checkers and successfully induce T2I models to generate NSFW images. Moreover, cross-model jailbreak effectiveness is an important aspect of evaluating attack performance. Therefore, in our subsequent experiments on other models, we adopt cross-model transfer attacks to reflect the proposed method’s cross-model attack capability. Fig. 3 shows the attack effect of

TABLE II: Comparison to baselines across two different prompt checkers. The bolded values are the highest performance.

T2I Model	Prompt Checker	Attack	Bypass-Text	Bypass-Img	Q16		MHSC	
					ASR-4	ASR-1	ASR-4	ASR-1
SDv1.4	NSFW-text-classifier	I2P	47.0%	68.0%	19.5%	6.5%	8.0%	2.5%
		QF-Attack	16.5%	80.0%	9.5%	2.0%	6.5%	1.5%
		SneakyPrompt	19.0%	81.5%	10.0%	5.0%	10.0%	3.5%
		FLIRT	13.0%	66.0%	7.0%	2.5%	3.5%	2.0%
		DiffZOO	17.5%	58.0%	7.5%	2.5%	5.0%	2.0%
		MMA-Diffusion	5.5%	64.5%	3.0%	1.5%	2.5%	1.0%
		DACA	60.0%	59.5%	20.5%	6.5%	4.5%	1.0%
		U3-Attack	10.5%	70.0%	8.0%	4.5%	5.5%	3.0%
		DREAM	18.0%	62.0%	13.0%	10.5%	15.0%	9.0%
		HTS-Attack	27.5%	74.0%	17.5%	8.0%	8.5%	4.5%
		TCBS-Attack	45.0%	82.0%	29.5%	13.5%	17.5%	10.0%
		SDv1.4	Detoxify	I2P	96.0%	68.0%	40.0%	18.5%
QF-Attack	71.0%			80.0%	37.5%	18.0%	24.5%	8.5%
SneakyPrompt	55.5%			81.5%	38.5%	19.5%	25.0%	9.5%
FLIRT	60.0%			66.0%	41.0%	20.0%	18.5%	8.5%
DiffZOO	68.5%			58.0%	29.0%	12.0%	21.5%	6.0%
MMA-Diffusion	58.0%			64.5%	29.5%	19.0%	26.5%	11.5%
DACA	98.5%			59.5%	41.0%	15.5%	11.0%	4.5%
U3-Attack	42.0%			70.0%	24.0%	16.0%	20.5%	6.0%
DREAM	84.0%			62.0%	45.0%	21.5%	29.5%	9.5%
HTS-Attack	75.0%			74.0%	44.5%	20.5%	29.0%	9.5%
TCBS-Attack	92.5%			82.0%	52.5%	22.0%	31.0%	14.5%

TCBS-Attack.

C. Experimental Results on Jailbreaking Securely Trained T2I Models

We repurpose the adversarial prompts obtained from previous experiments to conduct transfer attacks on two securely trained open-source T2I models: SafeGen and SLD. These models are specifically trained to remove unsafe concepts and suppress inappropriate images generated by other diffusion models. Similar to previous experiments, we integrate prompt checker (NSFW-text-classifier) and image safety checker for both securely trained T2I models.

Table III presents the comparative evaluation of TCBS-Attack and baseline methods against two securely trained T2I models. The results clearly indicate the superior performance of TCBS-Attack over other methods in terms of attack success rates.

For the SafeGen model, TCBS-Attack achieves the highest ASR-4 (20.0% on Q16, 10.0% on MHSC) and ASR-1 (8.0% on Q16, 6.0% on MHSC), surpassing baseline methods like HTS-Attack (16.5% ASR-4 on Q16), U3-Attack (4.0% ASR-1 on MHSC) and DREAM (7.5% ASR-1 on Q16). Similarly, for the SLD model, TCBS-Attack demonstrates notable effectiveness, achieving the highest ASR-4 of 17.0% and ASR-1 of 9.0%, significantly outperforming other baseline methods such as HTS-Attack(7.0% ASR-1), U3-Attack(2.0% ASR-1) and DREAM(15.5% ASR-4).

These results emphasize the robustness and effectiveness of TCBS-Attack, validating its superior capability to successfully induce securely trained T2I models to generate NSFW content despite their reinforced security training. Moreover, our results demonstrate the strong transferability of TCBS-Attack, effectively generalizing its adversarial prompts to bypass security mechanisms in various T2I model architectures.

TABLE III: Comparison to baselines across two securely trained T2I models. The bolded values are the highest performance.

T2I Model	Attack	Q16		MHSC	
		ASR-4	ASR-1	ASR-4	ASR-1
SafeGen	I2P	12.5%	4.5%	4.5%	2.5%
	QF-Attack	6.0%	2.0%	2.5%	1.5%
	SneakyPrompt	8.5%	4.0%	5.5%	4.0%
	FLIRT	6.0%	4.5%	3.0%	2.5%
	DiffZOO	3.0%	1.5%	2.0%	0.5%
	MMA-Diffusion	1.0%	0.0%	1.0%	0.5%
	DACA	13.5%	5.5%	3.0%	1.0%
	U3-Attack	6.5%	4.0%	5.5%	4.0%
	DREAM	13.0%	7.5%	9.0%	5.5%
	HTS-Attack	16.5%	6.0%	8.5%	4.0%
	TCBS-Attack	20.0%	8.0%	10.0%	6.0%
	SLD	I2P	7.0%	2.5%	11.0%
QF-Attack		2.0%	0.5%	6.0%	1.5%
SneakyPrompt		5.0%	1.5%	10.0%	4.0%
FLIRT		3.0%	1.0%	2.0%	1.0%
DiffZOO		2.0%	0.5%	5.0%	1.0%
MMA-Diffusion		2.0%	0.0%	2.0%	1.5%
DACA		6.0%	2.0%	4.0%	0.0%
U3-Attack		4.5%	1.5%	5.5%	2.0%
DREAM		8.0%	2.5%	15.5%	9.0%
HTS-Attack		6.0%	1.5%	12.5%	7.0%
TCBS-Attack		9.0%	3.0%	17.0%	9.0%

D. Experimental Results on Jailbreaking Online T2I Services

To further validate the real-world applicability of TCBS-Attack, we evaluate its effectiveness against commercial online T2I services, specifically DALL-E 3. Unlike open-source models, commercial T2I services typically employ advanced, multi-layered security measures that pose significant challenges for adversarial attacks. Considering the cost associated with commercial models, we conduct our experiments using 30 prompts from the UnsafeDiff dataset. Correspondingly,

I2P also selects 30 prompts from the matching categories. Additionally, the bypass rate in attacking DALL-E 3 represents the proportion of prompts successfully generating images.

TABLE IV: Comparison to baselines for online commercial model DALL-E 3. The bolded values are the highest performance.

Attack	Bypass	Q16		MHSC	
		ASR-4	ASR-1	ASR-4	ASR-1
I2P	66.7%	60.0%	33.3%	23.3%	10.0%
QF-Attack	93.3%	66.7%	53.3%	53.3%	36.7%
SneakyPrompt	76.7%	73.3%	33.3%	53.3%	33.3%
FLIRT	73.3%	66.7%	30.0%	46.7%	26.7%
DiffZOO	70.0%	73.3%	36.7%	50.0%	33.3%
MMA-Diffusion	96.7%	70.0%	50.0%	53.3%	30.0%
DACA	93.3%	40.0%	26.7%	26.7%	6.7%
U3-Attack	70.0%	60.0%	33.3%	50.0%	26.7%
DREAM	86.7%	66.7%	50.0%	56.7%	33.3%
HTS-Attack	86.7%	70.0%	53.3%	56.7%	36.7%
TCBS-Attack	93.3%	73.3%	56.7%	60.0%	36.7%

Table IV presents the comparative results between TCBS-Attack and baseline methods for the DALL-E 3 model. TCBS-Attack exhibits robust adversarial effectiveness with the highest ASR-4 rate of 73.33% and the highest ASR-1 rate of 56.67% on the Q16 detector, outperforming strong competitors such as U3-Attack (33.3% ASR-1, 60.0% ASR-4) and DREAM (50.0% ASR-1, 66.7% ASR-4). In the evaluation using the MHSC detector, TCBS-Attack achieves an ASR-4 rate of 60.00% and an ASR-1 rate of 36.67%, highlighting its capability to induce NSFW content generation despite DALL-E 3’s sophisticated security checks. These results underline the potency and versatility of TCBS-Attack, establishing it as a highly effective adversarial technique capable of challenging the security frameworks employed by leading commercial T2I services.

E. Ablation Study

Table V presents an ablation study conducted to evaluate the contributions of various constraints used in TCBS-Attack. We specifically consider three scenarios: removing the text constraint $F_{text}(\cdot)$, removing the image constraint $F_{img}(\cdot)$, and removing all constraints. TCBS-Attack disables the corresponding constraint functions during both the token search and token selection stages. Results clearly illustrate the significance of each constraint for enhancing attack performance.

TABLE V: Ablation Study. These experiments compare the performance of TCBS-Attack after ablating different constraints.

Attack	Bypass -Text	Bypass -Img	Q16		MHSC	
			ASR-4	ASR-1	ASR-4	ASR-1
TCBS-Attack	45.0%	82.0%	29.5%	13.5%	17.5%	10.0%
- $F_{text}(\cdot)$	24.5%	81.5%	13.5%	7.0%	10.0%	5.5%
- $F_{img}(\cdot)$	38.5%	80.0%	23.5%	9.5%	16.0%	6.0%
- All constraint	24.0%	79.0%	12.5%	6.5%	9.5%	4.0%

It is important to note that in the original design of TCBS-Attack, the token selection process prioritizes the image constraint $F_{img}(\cdot)$ first, followed by the text constraint

$F_{text}(\cdot)$, and finally the image similarity metric. When the image constraint is removed, TCBS-Attack adjusts its selection logic by first evaluating whether a candidate prompt satisfies the text constraint, and then ranking by image similarity. Conversely, when the text constraint is removed, the algorithm gives precedence to the image constraint, and only considers image similarity as a secondary criterion. In the case where both constraints are removed, TCBS-Attack ranks candidate prompts solely based on their image similarity to the target content.

This hierarchical constraint handling in the token selection phase ensures that the influence of each component can be independently evaluated, providing a clear understanding of the individual contributions of $F_{text}(\cdot)$ and $F_{img}(\cdot)$ to the overall attack effectiveness.

The fully constrained TCBS-Attack achieves the highest overall performance, exhibiting a high Bypass-Text rate of 45.0%, the highest Bypass-Img rate of 82.0%, and the best ASR-4 (29.5% on Q16) and ASR-1 (13.5% on Q16) scores. Removing the text constraint ($F_{text}(\cdot)$) significantly reduces the Bypass-Text rate to 24.5%, while moderately lowering the Bypass-Img rate to 81.5%, resulting in modest ASR performance. Similarly, when removing the image constraint ($F_{img}(\cdot)$), the Bypass-Text rate decreases to 38.5%, and Bypass-Img rate further declines to 80.0%, accompanied by intermediate ASR scores. The removal of all constraints dramatically undermines the attack’s effectiveness, leading to the lowest Bypass-Text rate of 24.0%, a Bypass-Img rate of 79.0%, and considerably diminished ASR performance, such as an ASR-1 of merely 6.5% on the Q16 detector. These results emphasize the critical importance of jointly applying text and image constraints, as this combination substantially enhances adversarial effectiveness against robust safety measures.

F. Query Budget Analysis

In TCBS-Attack, the population size is n and the number of iterations is T . We will perform additional queries on samples that successfully attack, so the theoretical maximum number of queries is $2 * n * T$, which is $10 * 50 \sim 20 * 50$ in our setting, while other query-based baselines requires 1000 queries. Empirically, our method issues an average of 532 queries per attack. We conducted supplementary experiments on the UnsafeDiff dataset with a fixed budget of 100 queries, comparing against other query-based baselines. The results are shown in Table VI.

TABLE VI: Query Budget Analysis.

Attack	Bypass -Text	Bypass -Img	Q16		MHSC	
			ASR-4	ASR-1	ASR-4	ASR-1
SneakyPrompt	50.0%	86.7%	36.7%	20.0%	26.6%	16.6%
HTS-Attack	73.3%	83.3%	56.6%	23.3%	46.6%	20.0%
TCBS-Attack	86.7%	93.3%	60.0%	23.3%	60.0%	36.6%

G. Sensitivity Analysis

Tables VII, VIII, and IX present the sensitivity analysis results for key parameters involved in TCBS-Attack, specifically

focusing on the relaxation margins for the image similarity constraint m_1 and NSFW score constraint m_2 and the number of similar tokens during token replacement k .

TABLE VII: Optimal parameter m_1 settings. These experiments compare different parameter m_1 settings.

Attack	Bypass -Text	Bypass -Img	Q16		MHSC	
			ASR-4	ASR-1	ASR-4	ASR-1
$m_1 = 0$	90.0%	86.7%	73.3%	36.7%	73.3%	43.3%
$m_1 = 0.025$	90.0%	83.3%	66.7%	40.0%	43.3%	26.7%
$m_1 = 0.05$	86.7%	90.0%	76.7%	40.0%	66.7%	43.3%
$m_1 = 0.075$	93.3%	90.0%	63.3%	33.3%	76.7%	40.0%
$m_1 = 0.1$	86.7%	90.0%	76.7%	40.0%	63.3%	40.00%

In conducting experiments on m_1 , we set $m_2 = 0.01$ and $k = 25$. The larger the value of m_1 , the broader the constraint boundary during token search; conversely, a smaller m_1 tightens the constraint boundary. Table VII demonstrates the sensitivity analysis for the parameter m_1 . The optimal performance appears at $m_1 = 0.05$, achieving the highest Bypass-Img rate of 90% and the highest ASR scores (40.00% ASR-1 for Q16 and 43.33% ASR-1 for MHSC). However, further increasing m_1 beyond 0.05 causes fluctuations in attack efficacy, indicating that $m_1 = 0.05$ provides a balanced constraint beneficial for consistent adversarial performance.

TABLE VIII: Optimal parameter m_2 settings. These experiments compare different parameter m_2 settings.

Attack	Bypass -Text	Bypass -Img	Q16		MHSC	
			ASR-4	ASR-1	ASR-4	ASR-1
$m_2 = 0.001$	86.7%	86.7%	76.7%	36.7%	60.0%	30.0%
$m_2 = 0.005$	90.0%	83.3%	80.0%	40.0%	56.7%	30.0%
$m_2 = 0.01$	86.7%	90.0%	76.7%	40.0%	66.7%	43.3%
$m_2 = 0.015$	86.7%	90.0%	63.3%	26.7%	60.0%	43.3%
$m_2 = 0.02$	80.0%	83.3%	56.7%	26.7%	56.7%	23.3%

In conducting experiments on m_2 , we set $m_1 = 0.05$ and $k = 25$. Table VIII demonstrates the sensitivity analysis for the parameter m_2 . A larger m_2 relaxes the image constraints during token search, whereas a smaller m_2 imposes stricter image constraints. The optimal setting identified is $m_2 = 0.01$, yielding the highest Bypass-Img rate of 90% and balanced ASR results (66.67% ASR-4 and 43.33% ASR-1 on MHSC).

TABLE IX: Optimal parameter k settings. These experiments compare different parameter k settings.

Attack	Bypass -Text	Bypass -Img	Q16		MHSC	
			ASR-4	ASR-1	ASR-4	ASR-1
$k = 5$	73.3%	80.0%	60.0%	30.0%	60.0%	20.0%
$k = 10$	83.3%	90.0%	56.7%	30.0%	60.0%	26.66%
$k = 15$	93.3%	90.0%	73.3%	33.3%	70.0%	33.3%
$k = 20$	93.3%	86.7%	80.0%	40.0%	70.0%	46.7%
$k = 25$	86.7%	90.0%	76.7%	40.0%	66.7%	43.3%
$k = 30$	83.3%	86.7%	63.3%	30.0%	66.7%	30.00%
$k = 35$	90.0%	93.3%	73.3%	36.7%	66.7%	43.3%

In conducting experiments on k , we set $m_1 = 0.05$ and $m_2 = 0.01$. A larger k reduces the textual similarity requirements during token search, which within certain limits can enhance the ability to bypass safety detectors. Table IX presents the sensitivity analysis results regarding the token

similarity parameter k . As k increases, the ability of TCBS-Attack to bypass both text and image checkers progressively improves. The best overall performance occurs at $k = 20$, with the highest ASR scores (80% ASR-4 for Q16 and 70% ASR-4 for MHSC) and Bypass-Text rate 93.33%. Further increasing k beyond 20 does not lead to substantial improvements and occasionally reduces effectiveness. This result highlights the critical role of the k parameter in effectively balancing token selection and semantic coherence to maximize attack performance.

V. CONCLUSIONS

In this work, we introduce TCBS-Attack, a token-level constraint boundary search method for jailbreaking Text-to-Image models. Unlike the existing approaches, TCBS-Attack leverages the decision boundaries of both prompt and image safety checkers, enabling effective generation of semantically coherent adversarial prompts. By framing the adversarial prompt search as a constrained optimization problem, TCBS-Attack achieves high attack success rates and output quality in finding adversarial prompts, underscoring the strengths of evolutionary search in navigating complex, high-dimensional prompt spaces. Our comprehensive evaluation demonstrated the effectiveness of TCBS-Attack in bypassing the full-chain defense of T2I systems, which consists of prompt-based and image-based defensive mechanisms as well as securely trained T2I models, in addition to challenging commercial online T2I services.

While TCBS-Attack has demonstrated its superiority in average performance, it still has shortcomings in search efficiency and generalization. Future research should strive to improve the efficiency and robustness of evolutionary attacks by incorporating advanced strategies to maintain diversity and escape local optima. In particular, there is significant potential in hybrid approaches that combine evolutionary algorithms with other intelligent optimization techniques to leverage their complementary strengths. Such integrations could lead to more efficient search processes and more robust, transferable adversarial prompt generation, further advancing the state of the art in understanding and testing the safety of T2I models.

ETHICAL STATEMENT

This work aims to identify and address security vulnerabilities in T2I models, with the goal of strengthening defenses rather than facilitating misuse. We encourage the research community and developers to apply our findings responsibly, prioritizing the prevention of malicious applications.

REFERENCES

- [1] R. Rombach, A. Blattmann, D. Lorenz, P. Esser, and B. Ommer, "High-resolution image synthesis with latent diffusion models," in *Proceedings of the IEEE/CVF conference on computer vision and pattern recognition*, 2022, pp. 10 684–10 695.
- [2] A. Ramesh, P. Dhariwal, A. Nichol, C. Chu, and M. Chen, "Hierarchical text-conditional image generation with clip latents," *arXiv preprint arXiv:2204.06125*, vol. 1, no. 2, p. 3, 2022.
- [3] Y. Qu, X. Shen, X. He, M. Backes, S. Zannettou, and Y. Zhang, "Unsafe diffusion: On the generation of unsafe images and hateful memes from text-to-image models," in *Proceedings of the 2023 ACM SIGSAC Conference on Computer and Communications Security*, 2023, pp. 3403–3417.

- [4] C. Saharia, W. Chan, S. Saxena, L. Li, J. Whang, E. L. Denton, K. Ghasemipour, R. Gontijo Lopes, B. Karagol Ayan, T. Salimans *et al.*, “Photorealistic text-to-image diffusion models with deep language understanding,” *Advances in neural information processing systems*, vol. 35, pp. 36 479–36 494, 2022.
- [5] P. Schramowski, M. Brack, B. Deiseroth, and K. Kersting, “Safe latent diffusion: Mitigating inappropriate degeneration in diffusion models,” in *Proceedings of the IEEE/CVF Conference on Computer Vision and Pattern Recognition*, 2023, pp. 22 522–22 531.
- [6] Y. Huang, L. Liang, T. Li, X. Jia, R. Wang, W. Miao, G. Pu, and Y. Liu, “Perception-guided jailbreak against text-to-image models,” *arXiv preprint arXiv:2408.10848*, 2024.
- [7] Y. Ma, S. Pang, Q. Guo, T. Wei, and Q. Guo, “Coljailbreak: Collaborative generation and editing for jailbreaking text-to-image deep generation,” *Advances in Neural Information Processing Systems*, vol. 37, pp. 60 335–60 358, 2024.
- [8] D. Yang, Y. Bai, X. Jia, Y. Liu, X. Cao, and W. Yu, “On the multi-modal vulnerability of diffusion models,” *arXiv preprint arXiv:2402.01369*, 2024.
- [9] A. Zou, Z. Wang, N. Carlini, M. Nasr, J. Z. Kolter, and M. Fredrikson, “Universal and transferable adversarial attacks on aligned language models,” *arXiv preprint arXiv:2307.15043*, 2023.
- [10] P. Chao, A. Robey, E. Dobriban, H. Hassani, G. J. Pappas, and E. Wong, “Jailbreaking black box large language models in twenty queries,” in *2025 IEEE Conference on Secure and Trustworthy Machine Learning (SaTML)*. IEEE, 2025, pp. 23–42.
- [11] H. Gao, H. Zhang, Y. Dong, and Z. Deng, “Evaluating the robustness of text-to-image diffusion models against real-world attacks,” *arXiv preprint arXiv:2306.13103*, 2023.
- [12] C. Liang, X. Wu, Y. Hua, J. Zhang, Y. Xue, T. Song, Z. Xue, R. Ma, and H. Guan, “Adversarial example does good: Preventing painting imitation from diffusion models via adversarial examples,” *arXiv preprint arXiv:2302.04578*, 2023.
- [13] Z. Wang, H. Wang, C. Tian, and Y. Jin, “Adversarial training of deep neural networks guided by texture and structural information,” in *Proceedings of the 31st ACM International Conference on Multimedia*, 2023, pp. 4958–4967.
- [14] Q. Liu, A. Kortylewski, Y. Bai, S. Bai, and A. Yuille, “Intriguing properties of text-guided diffusion models,” *arXiv preprint arXiv:2306.00974*, vol. 2, p. 4, 2023.
- [15] N. Maus, P. Chao, E. Wong, and J. Gardner, “Black box adversarial prompting for foundation models,” *arXiv preprint arXiv:2302.04237*, 2023.
- [16] H. Salman, A. Khaddaj, G. Leclerc, A. Ilyas, and A. Madry, “Raising the cost of malicious ai-powered image editing,” 2023. [Online]. Available: <https://arxiv.org/abs/2302.06588>
- [17] Y. Yang, R. Gao, X. Wang, T.-Y. Ho, N. Xu, and Q. Xu, “Mma-diffusion: Multimodal attack on diffusion models,” in *Proceedings of the IEEE/CVF Conference on Computer Vision and Pattern Recognition*, 2024, pp. 7737–7746.
- [18] S. Gao, X. Jia, Y. Huang, R. Duan, J. Gu, Y. Bai, Y. Liu, and Q. Guo, “Hts-attack: Heuristic token search for jailbreaking text-to-image models,” 2024. [Online]. Available: <https://arxiv.org/abs/2408.13896>
- [19] Z. Wang, H. Wang, C. Tian, and Y. Jin, “Efficient adversarial training with multi-fidelity optimization for robust neural network,” *Neurocomputing*, vol. 585, p. 127627, 2024.
- [20] S. Garg and G. Ramakrishnan, “Bae: Bert-based adversarial examples for text classification,” *arXiv preprint arXiv:2004.01970*, 2020.
- [21] Y. Huang, F. Juefei-Xu, Q. Guo, J. Zhang, Y. Wu, M. Hu, T. Li, G. Pu, and Y. Liu, “Personalization as a shortcut for few-shot backdoor attack against text-to-image diffusion models,” in *Proceedings of the AAAI Conference on Artificial Intelligence*, vol. 38, no. 19, 2024, pp. 21 169–21 178.
- [22] D. Jin, Z. Jin, J. T. Zhou, and P. Szolovits, “Is bert really robust? a strong baseline for natural language attack on text classification and entailment,” in *Proceedings of the AAAI conference on artificial intelligence*, vol. 34, no. 05, 2020, pp. 8018–8025.
- [23] Z. Kou, S. Pei, Y. Tian, and X. Zhan, “Character as pixels: A controllable prompt adversarial attacking framework for black-box text guided image generation models,” in *Proceedings of the Thirty-Second International Joint Conference on Artificial Intelligence (IJCAI-23)*. Proceedings of the Thirty-Second International Joint Conference on . . . , 2023.
- [24] Z. Wang, H. Wang, C. Tian, and Y. Jin, “Preventing catastrophic overfitting in fast adversarial training: A bi-level optimization perspective,” in *European Conference on Computer Vision*. Springer, 2024, pp. 144–160.
- [25] J. Ma, A. Cao, Z. Xiao, Y. Li, J. Zhang, C. Ye, and J. Zhao, “Jailbreaking prompt attack: A controllable adversarial attack against diffusion models,” *arXiv preprint arXiv:2404.02928*, 2024.
- [26] G. Apruzzese, H. S. Anderson, S. Dambra, D. Freeman, F. Pierazzi, and K. Roundy, ““real attackers don’t compute gradients”: bridging the gap between adversarial ml research and practice,” in *2023 IEEE Conference on Secure and Trustworthy Machine Learning (SaTML)*. IEEE, 2023, pp. 339–364.
- [27] W. Brendel, J. Rauber, and M. Bethge, “Decision-based adversarial attacks: Reliable attacks against black-box machine learning models,” *arXiv preprint arXiv:1712.04248*, 2017.
- [28] Y. Yang, B. Hui, H. Yuan, N. Gong, and Y. Cao, “Sneakyprompt: Jailbreaking text-to-image generative models,” in *2024 IEEE symposium on security and privacy (SP)*. IEEE, 2024, pp. 897–912.
- [29] P. Dang, X. Hu, D. Li, R. Zhang, Q. Guo, and K. Xu, “Diffzoo: A purely query-based black-box attack for red-teaming text-to-image generative model via zeroth order optimization,” in *Findings of the Association for Computational Linguistics: NAACL 2025*, 2025, pp. 17–31.
- [30] X. Liu, N. Xu, M. Chen, and C. Xiao, “Autodan: Generating stealthy jailbreak prompts on aligned large language models,” *arXiv preprint arXiv:2310.04451*, 2023.
- [31] J. Yu, X. Lin, Z. Yu, and X. Xing, “Gptfuzzer: Red teaming large language models with auto-generated jailbreak prompts,” *arXiv preprint arXiv:2309.10253*, 2023.
- [32] H. Liu, Y. Wu, S. Zhai, B. Yuan, and N. Zhang, “Riatig: Reliable and imperceptible adversarial text-to-image generation with natural prompts,” in *Proceedings of the IEEE/CVF Conference on Computer Vision and Pattern Recognition*, 2023, pp. 20 585–20 594.
- [33] J. Ho, A. Jain, and P. Abbeel, “Denoising diffusion probabilistic models,” *Advances in neural information processing systems*, vol. 33, pp. 6840–6851, 2020.
- [34] A. Radford, J. W. Kim, C. Hallacy, A. Ramesh, G. Goh, S. Agarwal, G. Sastry, A. Askell, P. Mishkin, J. Clark *et al.*, “Learning transferable visual models from natural language supervision,” in *International conference on machine learning*. Pmlr, 2021, pp. 8748–8763.
- [35] “Nsfw-text-classifier,” https://huggingface.co/michellejiejeli/NSFW_text_classifier, 2023, accessed: 2025-07-01.
- [36] Y. Deng and H. Chen, “Divide-and-conquer attack: Harnessing the power of llm to bypass safety filters of text-to-image models,” *arXiv preprint arXiv:2312.07130*, 2023.
- [37] C. Schuhmann, R. Beaumont, R. Vencu, C. Gordon, R. Wightman, M. Cherti, T. Coombes, A. Katta, C. Mullis, M. Wortsman *et al.*, “Laion-5b: An open large-scale dataset for training next generation image-text models,” *Advances in neural information processing systems*, vol. 35, pp. 25 278–25 294, 2022.
- [38] X. Li, Y. Yang, J. Deng, C. Yan, Y. Chen, X. Ji, and W. Xu, “Safegen: Mitigating unsafe content generation in text-to-image models,” *arXiv e-prints*, pp. arXiv–2404, 2024.
- [39] “Detoxify,” <https://github.com/unitaryai/detoxify>, 2022, accessed: 2025-07-01.
- [40] H. Zhuang, Y. Zhang, and S. Liu, “A pilot study of query-free adversarial attack against stable diffusion,” in *Proceedings of the IEEE/CVF Conference on Computer Vision and Pattern Recognition*, 2023, pp. 2385–2392.
- [41] N. Mehrabi, P. Goyal, C. Dupuy, Q. Hu, S. Ghosh, R. Zemel, K.-W. Chang, A. Galstyan, and R. Gupta, “Flirt: Feedback loop in-context red teaming,” *arXiv preprint arXiv:2308.04265*, 2023.
- [42] S. Yan, H. Wei, J. Fei, G. Yang, Z. Zhao, and Z. Wang, “Universally unfiltered and unseen: Input-agnostic multimodal jailbreaks against text-to-image model safeguards,” in *Proceedings of the 33rd ACM International Conference on Multimedia*, 2025, pp. 11 279–11 287.
- [43] B. Li, J. Wang, Y. Li, Z. Hu, L. Qi, J. Dong, R. Wang, H. Qiu, Z. Qin, and T. Zhang, “Dream: Scalable red teaming for text-to-image generative systems via distribution modeling,” *arXiv preprint arXiv:2507.16329*, 2025.
- [44] P. Schramowski, C. Tauchmann, and K. Kersting, “Can machines help us answering question 16 in datasheets, and in turn reflecting on inappropriate content?” in *Proceedings of the 2022 ACM conference on fairness, accountability, and transparency*, 2022, pp. 1350–1361.
- [45] A. Vaswani, N. Shazeer, N. Parmar, J. Uszkoreit, L. Jones, A. N. Gomez, E. Kaiser, and I. Polosukhin, “Attention is all you need,” *Advances in neural information processing systems*, vol. 30, 2017.
- [46] J. Devlin, M.-W. Chang, K. Lee, and K. Toutanova, “Bert: Pre-training of deep bidirectional transformers for language understanding,” in *Proceedings of the 2019 conference of the North American chapter of the association for computational linguistics: human language technologies, volume 1 (long and short papers)*, 2019, pp. 4171–4186.